Physics Letters B 797 (2019) 134805

Contents lists available at ScienceDirect

Physics Letters B

www.elsevier.com/locate/physletb

Nuclear charge radii of $^{62-80}$Zn and their dependence on cross-shell proton excitations

L. Xie [a], X.F. Yang [b,c,*], C. Wraith [d], C. Babcock [d], J. Bieroń [e], J. Billowes [a], M.L. Bissell [c,a], K. Blaum [f], B. Cheal [d], L. Filippin [h], K.T. Flanagan [a,i], R.F. Garcia Ruiz [c,a], W. Gins [c], G. Gaigalas [g], M. Godefroid [h], C. Gorges [k,l], L.K. Grob [j,k], H. Heylen [c,f,j], P. Jönsson [m], S. Kaufmann [k], M. Kowalska [j], J. Krämer [k], S. Malbrunot-Ettenauer [j], R. Neugart [f,l], G. Neyens [c,j], W. Nörtershäuser [k], T. Otsuka [n,o,c,p], J. Papuga [c], R. Sánchez [q], Y. Tsunoda [n], D.T. Yordanov [r]

[a] School of Physics and Astronomy, The University of Manchester, Manchester M13 9PL, United Kingdom
[b] School of Physics and State Key Laboratory of Nuclear Physics and Technology, Peking University, Beijing 100871, China
[c] KU Leuven, Instituut voor Kern- en Stralingsfysica, B-3001 Leuven, Belgium
[d] Oliver Lodge Laboratory, Oxford Street, University of Liverpool, Liverpool, L69 7ZE, United Kingdom
[e] Instytut Fizyki imienia Mariana Smoluchowskiego, Uniwersytet Jagielloński, ul. prof. Stanisława Łojasiewicza 11, Kraków, Poland
[f] Max-Planck-Institut für Kernphysik, D-69117 Heidelberg, Germany
[g] Institute of Theoretical Physics and Astronomy, Vilnius University, Sauletekio av. 3, LT-10222 Vilnius, Lithuania
[h] Chimie quantique et photophysique, Université libre de Bruxelles, B 1050 Brussels, Belgium
[i] Photon Science Institute Alan Turing Building, University of Manchester, Manchester M13 9PY, United Kingdom
[j] Experimental Physics Department, CERN, CH-1211 Geneva 23, Switzerland
[k] Institut für Kernphysik, TU Darmstadt, D-64289 Darmstadt, Germany
[l] Institut für Kernchemie, Universität Mainz, D-55128 Mainz, Germany
[m] School of Technology, Malmö University, Sweden
[n] Center for Nuclear Study, University of Tokyo, Hongo, Bunkyo-ku, Tokyo 113-0033, Japan
[o] Department of Physics, University of Tokyo, Hongo, Bunkyo-ku, Tokyo 113-0033, Japan
[p] National Superconducting Cyclotron Laboratory, Michigan State University, East Lansing, MI 48824, USA
[q] GSI Helmholtzzentrum für Schwerionenforschung, D-64291 Darmstadt, Germany
[r] Institute de Physique Nucléaire, CNRS-IN2P3, Université Paris-Sud, Université Paris-Saclay, 91406 Orsay, France

ARTICLE INFO

Article history:
Received 10 April 2019
Received in revised form 23 July 2019
Accepted 23 July 2019
Available online 25 July 2019
Editor: D.F. Geesaman

Keywords:
Zinc
Nuclear charge radii
Shell closure
Nuclear deformation
Correlations

ABSTRACT

Nuclear charge radii of $^{62-80}$Zn have been determined using collinear laser spectroscopy of bunched ion beams at CERN-ISOLDE. The subtle variations of observed charge radii, both within one isotope and along the full range of neutron numbers, are found to be well described in terms of the proton excitations across the $Z = 28$ shell gap, as predicted by large-scale shell model calculations. It comprehensively explains the changes in isomer-to-ground state mean square charge radii of $^{69-79}$Zn, the inversion of the odd-even staggering around $N = 40$ and the odd-even staggering systematics of the Zn charge radii. With two protons above $Z = 28$, the observed charge radii of the Zn isotopic chain show a cumulative effect of different aspects of nuclear structure including single particle structure, shell closure, correlations and deformations near the proposed doubly magic nuclei, ^{68}Ni and ^{78}Ni.

1. Introduction

The nuclear charge radius is one of the most fundamental properties of the atomic nucleus, and thus an important observable for understanding various aspects of nuclear structure: shell and subshell effects [1], configuration mixing [2], correlations [3] as well as nuclear deformation and shape coexistence [4,5]. Although efforts are made to successfully describe general trends of charge radii using various nuclear models, an accurate description of charge radii and their local variations, e.g. the odd-even staggering (OES), along a given isotopic chain remains a major challenge

* Corresponding author.
E-mail address: xiaofei.yang@pku.edu.cn (X.F. Yang).

https://doi.org/10.1016/j.physletb.2019.134805

[6–8]. For example, significant efforts have been made to establish a nuclear theory that accurately describes the parabolic shape of the charge radii and the pronounced OES in the Ca isotopic chain from $N = 20$ to $N = 28$ [9] and more recently from $N = 16$ to $N = 32$ [7,10,11].

The OES effect is ubiquitous but still remains to be an intriguing feature of nuclear charge radii, signalling a wealth of nuclear information. In general, the OES refers to the fact that charge radii of most odd-N isotopes are smaller than the average of adjacent even-N isotopes. This has been explained by the pairing effect. The unpaired neutron in an odd-N isotope blocks a certain orbit and thus suppresses the pair scattering [10,12,13], which in turn leads to a reduction in proton pair scattering. The resulting decrease of occupation probability of less bound proton orbits gives rise to a smaller charge radius. Therefore, the OES of charge radii should be sensitive to the subtle variation of proton excitations due to varying neutron numbers, and thus reflect the effect of correlations. Substantial experimental and theoretical investigations have been applied recently to understand the OES feature of nuclear charge radii, but mostly in specific regions where the OES effect is unusually large, such as for the light-mass $^{40-48}$Ca isotopes [10,9, 11], and more recently for the most notable example, known for many years, the neutron-deficient $^{177-185}$Hg isotopes [14]. However, these exceptional cases are not representative for the general case of much smaller OES in most other isotopic chains across the nuclear chart.

In the medium mass Ni region, the local fluctuation and OES of the nuclear charge radii are more typical, and thus suitable for a more fundamental understanding of the subtle correlations between minor changes of charge radii and proton cross-shell excitations. With two protons outside of the $Z = 28$ closed shell and neutrons between closed shells of $N = 28$ and 50, the Zn isotopes occupy a transitional region between single particle-like Ni isotopes and deformed Ge isotopes. Therefore, they are expected to exhibit the combined effects of shell closures and deformed shapes, which can be reflected in the various subtle variations of their charge radii.

This letter reports on the measurement of nuclear mean square charge radii of $^{62-80}$Zn isotopes, and a successful interpretation of their trend and their OES in terms of proton excitations across the $Z = 28$ shell gap. These have been calculated using the Monte Carlo Shell Model (MCSM) with the A3DA-m interaction in a full proton-neutron $pfg_{9/2}d_{5/2}$ model space [15]. This interaction was used before to successfully reproduce the magnetic and quadrupole moments of these Zn isotopes and their long-lived isomers [16], illustrating that the model correctly reproduces the ground and isomeric state wave functions.

2. Experimental method

The experiment was performed at the COLLAPS setup [17] at ISOLDE-CERN. The Zn isotopes were produced from a thick UC_x target bombarded by a 1.4 GeV proton beam. The Zn isotopes released from the target were selectively ionised by the resonance ionisation laser ion source RILIS [18]. Extracted Zn^+ ions were accelerated to 30 keV and mass separated. The ions were delivered to the COLLAPS setup typically as 5 µs bunches after 200 ms accumulation time in the radio frequency quadrupole cooler and buncher ISCOOL [19,20]. The ions were neutralised by passage through sodium vapour in a charge exchange cell (CEC). The $4s4p\ ^3P_2^o$ metastable state of Zn I was populated in the neutralisation process, from where the atoms were resonantly excited to the $4s5s\ ^3S_1$ state by a laser beam from a frequency-doubled cw Ti:sapphire laser. The laser wavelength was locked at 480.7254 nm to match the Doppler shifted transition. Four photomultipliers installed at the detection region were used to record the emitted fluorescence photons from the laser-excited atoms as a function of a tuning voltage applied to the CEC. More details about the experimental set-up can be found in [5,16].

3. Experimental results

The hyperfine spectra of the odd-mass $^{63-79}$Zn isotopes have been reported in [16], while the zero nuclear spin of even Zn isotopes results in a single resonance spectrum. The observed hyperfine spectra were fitted using a χ^2 minimisation procedure, generating the hyperfine-structure A and B parameters of the odd-mass isotopes and isomers (as reported in [16]), and the centroid frequency ν of all $^{62-80}$Zn isotopes and isomers. The isotope shifts (IS: $\delta\nu^{68,A} = \nu^A - \nu^{68}$) were calculated with respect to the centroid of ^{68}Zn (ν^{68}), as presented in Table 1. A systematic uncertainty on the laser frequency observed by the moving ions, which originates from the voltage uncertainty (about 0.033%) on the starting potential (30 kV) at ISCOOL, has been introduced.

The changes in mean square charge radii $\delta\langle r^2\rangle$ were obtained from the IS based on the equation [22,23]

$$\delta\nu^{68,A} = K_{\mathrm{MS}}\frac{m_A - m_{68}}{m_A m_{68}} + F\delta\langle r^2\rangle^{68,A}. \quad (1)$$

Here K_{MS} and F are the atomic mass-shift and field-shift factors, respectively, of the atomic transition used in this measurement. Since the mean square charge radii of five stable Zn isotopes are known experimentally from a combined analysis of electron scattering and muonic x-ray data [24], a King-plot procedure using these experimental $\delta\langle r^2\rangle_{\mu e}$ can be performed to evaluate the atomic factors [24–26]. As these evaluations of F and K_{MS} factors have rather large error bars in the case of Zn [25,24], we take advantage of the recent progress in multi-configuration Dirac-Hartree-Fock (MCDHF) calculations based on an ab-initio approach to better quantify the F-factor [27]. This method has indeed proven to be very successful in calculating the F-factor for a range of elements [3,28–31]. For the case of Zn, Filippin et al., [32] have explored different electron correlations in a systematic way, in order to optimise their computational strategy. They provide a final F-factor, $F = +346(3)$ MHz/fm^2, in which the uncertainty is estimated based on the variation of the three different correlation models [32]. However, the calculated mass shift, $K_{\mathrm{MS}} = +14(7)$ GHz u, in common with other systems [3,29], has a significant discrepancy with the value deduced from a King-plot analysis, leading to charge radii which do not conform to regional systematics. As with the case of Cu ($Z = 29$) [3] and Ga ($Z = 31$) [29], we therefore use the calculated value $F = +346(35)$ MHz/fm^2 with a 10% uncertainty, and we use the King plot with non-optical data $\delta\langle r^2\rangle_{\mu e}$ of stable isotopes [24] to extract the value of $K_{\mathrm{MS}} = +49(17)$ GHz u. In this analysis, the F-value from the calculation was used as a constraint but allowed to vary within the 10% uncertainty. With these empirical atomic factors, the changes in mean square charge radii $\delta\langle r^2\rangle$ for $^{62-80}$Zn are extracted, as shown in Table 1 and in Fig. 1a. The systematic error quoted for $\delta\langle r^2\rangle$ arises mainly from the uncertainty in the atomic factors after removing the correlations between K_{MS} and F during the King-plot procedure [8]. The systematic error on the IS, due to the uncertainty of the beam energy, has no effect on the final $\delta\langle r^2\rangle$ systematic error as the atomic factors allow their influence to be cancelled through the King-plot procedure. By comparison with the Cu and Ga isotopic chains shown in Fig. 1a, the Zn radii are consistent with the general trend of charge radii of neighbouring isotopes, while a deviation from the trend is observed if K_{MS} from MCDHF is used to extract the radii (black dots).

Table 1
Isotope shifts and changes in mean square charge radii of $^{62-80}$Zn $\delta\langle r^2\rangle^{68,A}$. Statistical errors are shown in curved brackets. Systematic errors in square brackets arise primarily from the uncertainty on the beam energy (for isotope shifts) and on atomic factors K_{MS} and F (for radii), respectively.

A	I^{π}	$\delta\nu^{68,A}$ (MHz)	$\delta\langle r^2\rangle^{68,A}$ (fm^2)
62	0^+	−239.5(11)[99]	−0.493(3)[52]
63	$3/2^-$	−191.2(32)[87]	−0.389(9)[43]
64	0^+	−141.2(12)[66]	−0.279(4)[34]
65	$5/2^-$	−121.8(23)[51]	−0.257(7)[25]
66	0^+	−63.6(15)[38]	−0.121(4)[16]
67	$5/2^-$	−41.4(21)[16]	−0.089(6)[8]
68	0^+	0	0
69	$1/2^-$	19.5(20)[15]	0.026(6)[9]
69^m	$9/2^+$	35.7(11)[15]	0.073(3)[8]
70	0^+	69.5(9)[29]	0.142(3)[15]
71	$1/2^-$	108.8(24)[44]	0.227(7)[23]
71^m	$9/2^+$	96.3(11)[43]	0.191(3)[23]
72	0^+	140.6(10)[57]	0.292(3)[30]
73	$1/2^-$	158.9(12)[71]	0.318(3)[37]
73^m	$5/2^+$	160.4(19)[71]	0.322(6)[37]
74	0^+	187.9(13)[83]	0.375(4)[44]
75	$7/2^+$	187.7(10)[96]	0.349(3)[51]
75^m	$1/2^-$	195.8(21)[96]	0.373(6)[51]
76	0^+	221.3(14)[108]	0.421(4)[57]
77	$7/2^+$	236.0(16)[120]	0.440(5)[64]
77^m	$1/2^-$	241.2(38)[120]	0.455(11)[64]
78	0^+	255.7(11)[131]	0.474(3)[70]
79	$9/2^+$	259.3(10)[142]	0.461(3)[77]
79^m	$1/2^+$	320.6(29)[142]	0.639(8)[75]
80	0^+	268.4(12)[161]	0.465(4)[84]

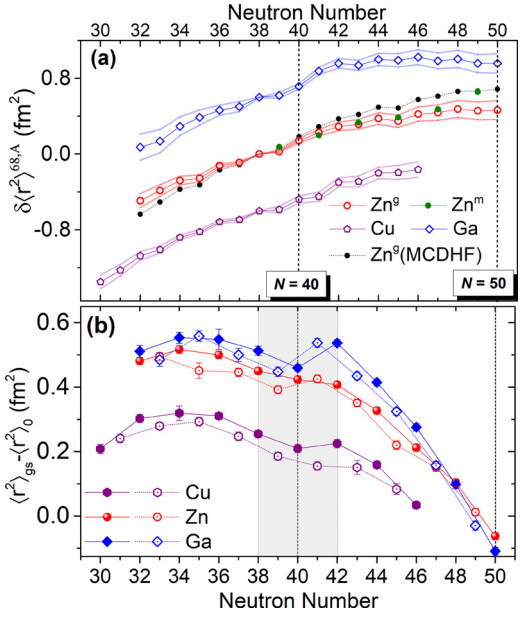

Fig. 1. (a) Changes in mean square charge radii for the Zn isotopes compared with neighbouring Cu and Ga isotopic chains, which are vertically offset by ± 0.6 fm^2 for clarity. The black dots present the Zn radii extracted by using the K_{MS} from MCDHF calculations. (b) Experimental $\langle r^2\rangle$ for ground states of the Cu, Zn and Ga isotopes with the spherical volume contribution $\langle r^2\rangle_0$ from the droplet model subtracted [21].

4. Discussion

The (sub-) shell effect has been much investigated in this region, as discussed for the Cu and Ga isotopes [3,29]. For this purpose, we plot the 'residual' $\langle r^2\rangle$ of Cu, Zn, Ga isotopes after subtracting the spherical volume contribution $\langle r^2\rangle_0$ of the droplet model [21], as shown in Fig. 1b. The general parabolic shape of the 'residual' charge radii $\langle r^2\rangle - \langle r^2\rangle_0$ demonstrates the shell effect expected near $N = 28$ and $N = 50$, while the local minimum of the $\langle r^2\rangle - \langle r^2\rangle_0$ around $N = 40$, which has been attributed to a weak subshell effect for Cu [3], is much weaker for ^{70}Zn than for ^{69}Cu. The apparent 'dip' in the Ga isotopic chain at $N = 40$ is not due to the subshell effect, but arises from an inversion of the OES [3,29,33] and onset of deformation appearing above $N = 40$, as observed in the nuclear moments [34]. Thus the Zn radii confirm the consistent picture of the $N = 40$ subshell effect which quickly disappears when going away from $Z = 28$, as described by various experimental observables: magnetic and quadrupole moments [16,35–37], charge radii [3,29], nuclear masses [38,39], $E(2^+)$ excitation energies, and $B(E2)$ transition rates [40–43].

In addition to the observed disappearing shell effect, nucleon correlations or deformation should contribute to the 'residual' charge radii. As an example, a different behaviour of OES below and above $N = 40$ is observed for the three isotopic chains (shaded region in Fig. 1b). An inversion of the normal OES around $N = 40$ is clearly observed for Ga isotopes and hinted for Zn isotopes, but not apparent in the Cu isotopes. The slight increase in collectivity above $N = 40$, observed in the experimental quadrupole moments of the odd Zn isotopes, and the $B(E2;\uparrow)$ of even ones, is considered as one possible explanation [16,44,45,43]. An increase in deformation was also observed in the Ga isotopic chain [37] but not in the Cu isotopic chain [46].

To assess the contribution of correlations to the experimental charge radii, one can attempt to describe $\delta\langle r^2\rangle$ in terms of changes in proton orbit occupation probabilities resulting from cross-shell excitations. This approach has been adopted recently to explain the pronounced OES in the charge radii of the Hg isotopes [14]. A naive shell model picture will predict a constant proton number of 2 above the $Z = 28$ closed shell for Zn. However, it is known that the proton single particle levels are modified with increasing neutron numbers [47]. This gives rise to proton excitations across the $Z = 28$ shell gap, as discussed recently for the Cu isotopes [35,48]. Such excitations can be quantified from the shell model with a large model space. MCSM using the A3DA-m interaction [15] in a $fpg_{9/2}d_{5/2}$ model space has been widely used in the Ni region [16,44,35] to describe nuclear moments. In order to examine the sensitivity of charge radii to proton excitations across $Z = 28$, the calculated proton occupations for the $1/2^-$ and high-spin states of $^{69-79}$Zn are presented in Fig. 2b. The trend in these proton occupations is compared to the trend in the experimental $\delta\langle r^2\rangle$ in Fig. 2a. For the $I = 1/2^+$ isomeric state of ^{79}Zn, since a large part of the contribution to its configuration comes from the neutron intruder $s_{1/2}$ orbit which is out of the model space (proton and neutron in $pfd_{5/2}g_{9/2}$ shells) of the A3DA-m interaction [5,16], we have used a newly developed $pfsdg$-full interaction [49] to calculate the proton occupation number (see the blue diamond in Fig. 2b). This new interaction, with an extended model space in the full proton and neutron $pfsdg$ shell, predicts the nuclear moment of this $1/2^+$ state in ^{79}Zn as $\mu_{\text{pfsdg-full}} = -1.05\ \mu_N$, in good agreement with the experimental value $\mu_{\text{exp}} = -1.018(1)\ \mu_N$ [5].

Fig. 2 clearly shows a qualitative relationship between the proton occupation above $Z = 28$ and the relative nuclear size of ground and isomeric states in $^{69-77}$Zn. The state with a larger proton occupation coincides with the state of larger size. In particular, it solves a puzzle visible in Fig. 2a: the charge radii of the $I = 1/2^-$ and $I = 9/2^+$ states are in the opposite order for ^{69}Zn and ^{71}Zn although they share same spins and similar magnetic moments [16].

Furthermore, the sensitivity of local changes of charge radii to the proton occupation can be explored qualitatively along the whole Zn isotopic chain. For this purpose, the proton excitations across the $Z = 28$ major shell closure for all $^{62-80}$Zn isotopes are converted into changes in the charge radii, $\delta\langle r^2\rangle_{(\text{p.occ})}$, by

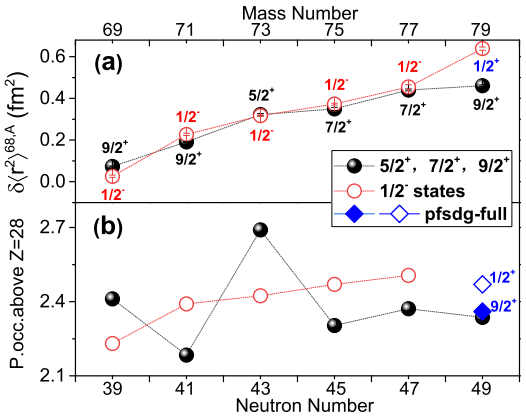

Fig. 2. (a) Experimental $\delta\langle r^2\rangle$ compared with (b) proton occupation numbers above $Z = 28$ calculated from A3DA-m interaction for both positive parity states and $1/2^-$ states in $^{69-79}$Zn. Note that the proton occupation number for the $1/2^+$ isomer in ^{79}Zn is calculated with a new interaction *pfsdg*-full (see the blue diamond in b), due to the model space limit of A3DA-m interaction.

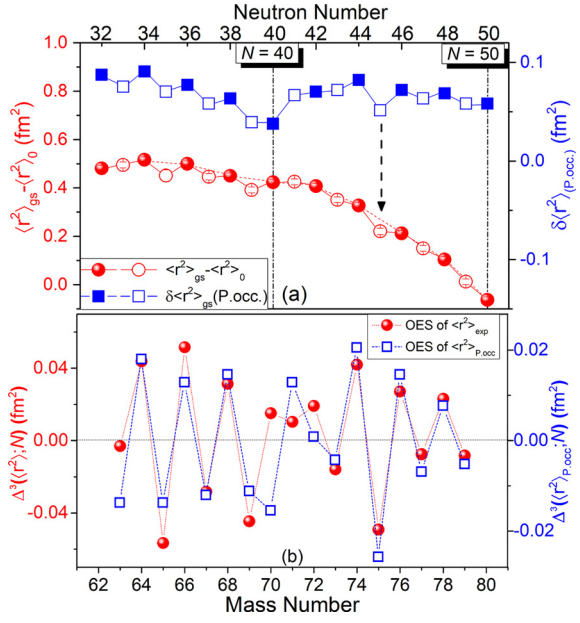

Fig. 3. (a) The $\delta\langle r^2\rangle$ of $^{62-80}$Zn (blue square) scaled from the excited proton across $Z = 28$ (see text for details) compared with the 'residual' charge radii $\langle r^2\rangle - \langle r^2\rangle_0$ (red circle) taken from Fig. 1b. The error bars are smaller than the symbols. (b) The odd-even staggering (OES) of experimental charge radii (red circle) and the charge radii (blue circle) scaled from the proton occupations, as shown in (a), see text for details.

multiplying the proton excitations with a constant scaling factor, $f = 0.172(7)$, estimated from the ratio of the isomer shift ($\delta\langle r^2\rangle^{g,m}$) and the occupation differences of ground and isomeric states ($\delta p^{g,m}$) of $^{69-77}$Zn from Fig. 2. Note that the value for ^{73}Zn is not taken into account for the determination of f, due to its large deformation [44]. The results of this procedure are shown by the blue squares in Fig. 3a, compared with the 'residual' charge radii $\langle r^2\rangle - \langle r^2\rangle_0$ of $^{62-80}$Zn (red circle). This scaling is made under the assumption that the differences in radii between the proton orbits $pf_{5/2}g_{9/2}d_{5/2}$ are negligible compared to the difference with the $f_{7/2}$ orbit below the $Z = 28$ shell gap.

Although a fully quantitative analysis is impossible without detailed calculations of the radii of the specific single particle orbits, the magnitude of the odd-even effect in experimental charge radii agrees with that from proton orbit occupation probabilities, as can be seen in Fig. 3a. Subtle changes in proton occupations above $Z = 28$ have noticeable effects on mean square charge radii along the entire Zn isotopic chain. For instance, in the mid-shell between $N = 40$ and $N = 50$, there is a reduction in the experimental charge radius at $N = 45$ (black arrow in Fig. 3a) compared to adjacent isotopes, which can be understood from the sudden decrease in proton excitations. Approaching the $N = 50$ neutron closed shell, the cross-shell excitations are suppressed as expected (and as observed also for the Cu isotopes [35]), resulting in a reduction of the OES, as reflected in the experimental charge radii. Around $N = 40$, the aforementioned inversion of the OES of radii in Fig. 1b) is also nicely described by the changes of proton occupation. There is only one exception observed around $N = 33$, where radii scaled from the proton occupation exhibits a usual odd-even effect while this is nearly invisible in the experimental charge radii. This is possibly due to the fact that the $3/2^-$ ground state in ^{63}Zn has a rather mixed configuration from neutron $f_{5/2}$ and $p_{3/2}$, as concluded from its magnetic moment and large quadrupole moment [16]. However, the A3DA-m calculation failed to reproduce the experimental magnetic moment of ^{63}Zn [16], $\mu_{\rm exp} = -0.282(1)\ \mu_N$ and $\mu_{\rm A3DA\text{-}m} = +0.110\ \mu_N$, which may be the origin of the discrepancy.

To better visualise the odd-even effect in the charge radii, the experimental OES is presented in Fig. 3b with solid circles, as the difference $\Delta^3(\langle r^2\rangle, N)$ between the radius of the isotope with neutron number N and the mean value of the radii of its neighbours with neutron numbers of $N+1$, $N-1$, as quantified with [50,51]:

$$\Delta^3(\langle r^2\rangle, N) = \langle r^2\rangle^N - \frac{1}{2}(\langle r^2\rangle^{N-1} + \langle r^2\rangle^{N+1}). \quad (2)$$

A value $\Delta^3(\langle r^2\rangle, N) > 0$ for an odd-N isotope represents an inversion of the normal OES behaviour. The hinted inversion in the OES at $N = 41$ is clearly visible in this representation. To understand its origin, we present in Fig. 3b also the calculated $\Delta^3(\langle r^2\rangle, N)$ with open squares, extracted from the calculated radii using the proton occupations above $Z = 28$ (the blue squares in Fig. 3a). The OES from the calculated radii shows also an inversion in the OES at $N = 41$. As these calculated radii were obtained from scaling of the proton excitation across $Z = 28$ (Fig. 2b), this suggests that indeed the inverted OES effect is related to changes in the proton excitations across $Z = 28$. Note that the low proton excitations around $N = 40$ (blue square in Fig. 3a) led to a wrong sign of $\Delta^3(\langle r^2\rangle, N)$ at $N = 40$ (blue square in Fig. 3b). Due to the parity change between two major shells at $N = 40$, the neutron excitations are suppressed, as recently demonstrated theoretically for the ^{68}Ni and ^{69}Cu [52], which in its turn lead to a suppression of the correlated proton excitations. However, such effect is probably overestimated in the MCSM calculation for the Zn isotope at $N = 40$. Nevertheless, the OES of the experimental nuclear charge radii and scaled charge radii share a similar relative amplitude over the whole Zn isotopic chain, confirming the strong connection between proton excitations across $Z = 28$ and nuclear charge radii. Fig. 3b also illustrates that, around the neutron mid-shell, the OES of charge radii calculated from proton occupations is pronounced, e.g. around $N = 34$ and $N = 45$, the middle shell of neutron $f_{5/2}$ and $g_{9/2}$ orbits, respectively. This phenomenon is also highlighted in the OES of experimental charge radii. In contrast, approaching the closed shell $N = 50$, the OES is suppressed for both experimental charge radii and scaled radii from proton occupations.

5. Summary and conclusion

In summary, the changes in mean square charge radii of $^{62-80}$Zn were extracted by laser spectroscopy. The variations in the charge radii of $^{62-80}$Zn were described in terms of proton

excitations across the $Z = 28$ shell gap. The proton excitation probability comprehensively explains the local variations of charge radii, such as the size change between the isomeric and ground states in $^{69-79}$Zn, the unusual inversion of the normal OES around $N = 40$, and the OES of the charge radii of $^{62-80}$Zn. This observation provides strong evidence that the charge radius is a sensitive reflection of the cross-shell proton excitations (which are strongly correlated to the neutron numbers), offering a new approach for the interpretation of nuclear charge radii.

Acknowledgements

We acknowledge the support of the ISOLDE collaboration and technical teams. This work was supported by the National Key R&D Program of China (Contract No. 2018YFA0404403), the National Natural Science Foundation of China (No.11875073), the UK Science and Technology Facilities Council grants ST/L005670/1 and ST/L005794/1, the JSPS and FWO under the Japan-Belgium Research Cooperative Program, the IAP-project P7/12, the FWO-Vlaanderen, GOA grant 15/010 from KU Leuven, the BMBF Contract No. 05P15RDCIA, the Max-Planck Society, the Helmholtz International Center for FAIR (HIC for FAIR), the EU FP7 via ENSAR No. 262010, the HPCI Strategic Program (The origin of matter and the universe) and “Priority Issue on post-K computer” (Elucidation of the Fundamental Laws and Evolution of the Universe) from MEXT and JICFuS, and the FWO-FNRS Excellence of Science Programme (Grant No. EOS-O022818F). The MCSM calculations were performed on the K computer at RIKEN AICS (hp150224, hp160211, hp170230).

References

[1] K. Kreim, et al., Phys. Lett. B 731 (2014) 97.
[2] H. De Witte, et al., Phys. Rev. Lett. 98 (2007) 112502.
[3] M.L. Bissell, et al., Phys. Rev. C 93 (2016) 064318.
[4] B. Cheal, et al., Phys. Lett. B 645 (2007) 133.
[5] X.F. Yang, et al., Phys. Rev. Lett. 116 (2016) 182502.
[6] A. Ekström, et al., Phys. Rev. C 91 (2015) 051301.
[7] R.F. Garcia Ruiz, et al., Nat. Phys. 12 (2016) 594.
[8] M. Hammen, et al., Phys. Rev. Lett. 121 (2018) 102501.
[9] E. Caurier, et al., Phys. Lett. B 522 (2001) 240.
[10] P.-G. Reinhard, W. Nazarewicz, Phys. Rev. C 95 (2017) 064328.
[11] A. Miller, et al., Nat. Phys. 15 (2019) 432.
[12] D. Zawischa, Phys. Lett. B 115 (1985) 309.
[13] M.L. Bissell, et al., Phys. Rev. Lett. 113 (2014) 052502.
[14] B. Marsh, et al., Nat. Phys. 14 (2018) 1163.
[15] Y. Tsunoda, et al., Phys. Rev. C 89 (2014) 031301.
[16] C. Wraith, et al., Phys. Lett. B 771 (2017) 385.
[17] R. Neugart, et al., J. Phys. G, Nucl. Part. Phys. 44 (2017) 064002.
[18] V.N. Fedosseev, et al., Rev. Sci. Instrum. 83 (2012) 02A903.
[19] E. Mané, et al., Eur. Phys. J. A 42 (3) (2009) 503.
[20] H. Franberg, et al., Nucl. Instrum. Methods B 266 (2008) 4502–4504.
[21] D. Berdichevsky, F. Tondeur, Z. Phys. A 322 (1985) 141.
[22] B. Cheal, K.T. Flanagan, J. Phys. G, Nucl. Part. Phys. 37 (2010) 113101.
[23] P. Campbell, et al., Prog. Part. Nucl. Phys. 86 (2016) 127.
[24] C.J. Foot, et al., Proc. R. Soc. Lond. A 384 (1982) 205.
[25] G. Fricke, K. Heilig, Nuclear Charge Radii, 1st edition, Springer-Verlag Berlin Heidelberg, 2004.
[26] P. Campbell, et al., J. Phys. B, At. Mol. Opt. Phys. 30 (1997) 2351.
[27] P. Jönsson, et al., Comput. Phys. Commun. 184 (2013) 2197–2203.
[28] K. Minamisono, et al., Phys. Rev. Lett. 117 (2016) 252501.
[29] T.J. Procter, et al., Phys. Rev. C 86 (2012) 034329.
[30] H. Heylen, et al., Phys. Rev. C 94 (2016) 054321.
[31] L.J. Vormawah, et al., Phys. Rev. A 97 (2018) 042504.
[32] L. Filippin, et al., Phys. Rev. A 96 (2017) 042502.
[33] G.J. Farooq-Smith, et al., Phys. Rev. C 96 (2017) 044324.
[34] B. Cheal, et al., Phys. Rev. Lett. 104 (2010) 252502.
[35] R. de Groote, et al., Phys. Rev. C 96 (2017) 041302(R).
[36] K.T. Flanagan, et al., Phys. Rev. Lett. 103 (2009) 142501.
[37] B. Cheal, et al., Phys. Rev. Lett. 104 (2010) 252502.
[38] C. Guénaut, et al., Phys. Rev. C 75 (2007) 044303.
[39] S. Rahaman, et al., Eur. Phys. J. A 34 (2007) 5.
[40] N. Aoi, et al., Phys. Lett. B 692 (2010) 302.
[41] C.J. Chiara, et al., Phys. Rev. C 84 (2011) 037304.
[42] O. Perru, et al., Phys. Rev. Lett. 96 (2006) 232501.
[43] C. Louchart, et al., Phys. Rev. C 87 (2013) 054302.
[44] X.F. Yang, et al., Phys. Rev. C 97 (2018) 044324.
[45] M. Niikura, et al., Phys. Rev. C 85 (2012) 054321.
[46] P. Vingerhoets, et al., Phys. Rev. C 82 (2010) 064311.
[47] T. Otsuka, et al., Phys. Rev. Lett. 95 (2005) 232502.
[48] T. Otsuka, et al., Phys. Rev. Lett. 104 (2010) 012501.
[49] Y. Tsunoda, T. Otsuka, private communication.
[50] K. Lynch, et al., Phys. Rev. C 97 (2018) 024309.
[51] P. Lievens, et al., Europhys. Lett. 33 (1996) 11.
[52] Y. Ichikawa, et al., Nat. Phys. 15 (2019) 321.